HIGHER ORDER MODULATION AND THE EFFICIENT SAMPLING ALGORITHM FOR TIME VARIANT SIGNAL

Jian-Jiun Ding, Soo Chang Pei, and Ting Yu Ko

Department of Electrical Engineering, National Taiwan University,
No. 1, Sec. 4, Roosevelt Rd., 10617, Taipei, Taiwan,
TEL: +886-2-23635251-321, Fax: +886-2-23671909, Email: djj@cc.ee.ntu.edu.tw, pei@cc.ee.ntu.edu.tw, jkngel.ko@gmail.com

ABSTRACT

From the sampling theory, if the bandwidth of a signal is small, then the sampling interval can be very large. In this paper, a higher order modulation scheme is proposed to minimize the bandwidth of a signal. Then, combining the proposed high order modulation with the fractional Fourier transform and time-frequency analysis, a new sampling algorithm is presented. The proposed sampling algorithm can minimize the area of a signal in the time-frequency domain and much reduce the number of sampling points. Simulation results show that, when using the proposed sampling algorithm, the amount of data required for recording a signal can be much less. The proposed sampling algorithm is especially efficient for sampling a time variant signal, such as the voice of an animal and the speech signal.

Index Terms— Signal sampling, time-frequency analysis, time variant signal analysis, spectrogram, modulation

1. INTRODUCTION

From Shannon's sampling theory [1], to sample a signal, the sampling frequency should be larger than the Nyquist rate:

$$f_s \geq F \qquad \text{i.e.,} \qquad \Delta \leq \frac{1}{F} \tag{1}$$

where f_s is the sampling frequency, $\Delta = 1/f_s$ is the sampling interval, and F is the total bandwidth (including the positive and the negative frequency parts) of the signal. From (1), it can be seen that the upper bound of the sampling interval is determined by the bandwidth of a signal.

Moreover, suppose that the support of a signal is T:

$$x(t) \cong 0 \quad \text{for } t < t_0 \text{ and } t > t_0 + T. \tag{2}$$

If its bandwidth is F, from (1), the number of sampling points required for $x(t)$ is

$$\frac{T}{\Delta_t} \geq TF \ . \tag{3}$$

Therefore, the ***TF* value** determines the lower bound of sampling points.

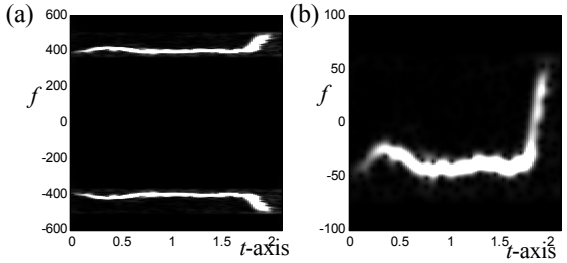

Figure 1 – (a) The STFT of the fundamental harmonic part of a whale voice signal in [2]. (***TF* value = 2100**) (b) The STFT of $x_1(t)$ defined in (5). $x_1(t)$ is the modulated analytic signal for the whale voice signal in (a) (***TF* value = 210**).

For example, Fig. 1(a) is the short-time Fourier transform (STFT) [3][4] of the fundamental harmonic part of a whale voice signal obtained from [2]. The STFT is one of the methods to transform a signal into the time-frequency domain. In Fig. 1(a), one can be seen that the signal is 2.1 second long and the bandwidth of the signal is about 1000 Hz. Thus, the number of sampling points required for the signal should be larger than $TF = 2.1 \times 1000 =$ **2100**.

Since the lower bound of the number of sampling points is determined by TF, i.e., the "rectangular area" of the signal in the time-frequency plane, to minimize the number of sampling points, one can try to reduce the TF value. There are several ways to accomplish it. For example, one can first convert the signal into the analytic signal form [1]:

$$x_a(t) = x(t) + jx_H(t) \tag{4}$$

where $x_H(t)$ is the Hilbert transform of $x(t)$. Note that $X_a(f) = X(f)$ for $f > 0$ and $X_a(f) = 0$ for $f < 0$. Then, the conventional modulation operation is performed for $x_a(t)$ [1]:

$$x_1(t) = e^{-j2\pi f_1 t} x_a(t). \tag{5}$$

For example, for the whale voice signal whose STFT is as in Fig. 1(a), after applying the analytic signal conversion and the conventional modulation operations as in (4) and (5) (f_1 is chosen as 440), the STFT of the resultant signal $x_1(t)$ is as in Fig. 1(b). It can be seen that the bandwidth of $x_1(t)$ is about 100 Hz (from -50Hz to 50Hz) and the TF value (i.e., the lower bound of the number of sampling points) is reduced to $2.1 \times 100 =$ **210**.

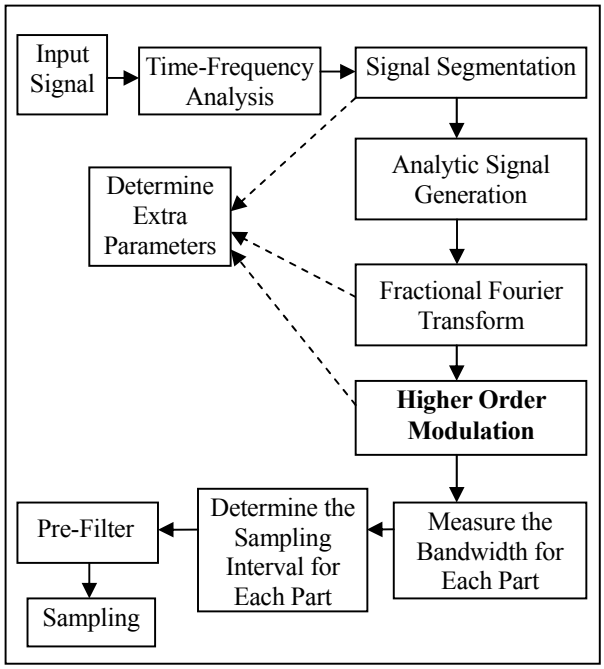

Figure 2 – The flowchart of the proposed sampling algorithm.

In this paper, we introduce an efficient signal sampling algorithm that is based on the proposed high order modulation operation. That is, instead of the conventional modulation operation in (5), the higher order exponential function is adopted for modulation. Moreover, the fractional Fourier transform [5], the signal segmentation technique, and the pre-filter for reducing the aliasing effect before sampling [1] are also applied in our sampling procedure. The whole procedure of the proposed sampling algorithm is plotted in Fig. 2. The simulation results show that the proposed sampling algorithm is especially efficient for sampling a time-variant signal, such as the speech signal and the voice of an animal.

2. HIGHER ORDER MODULATION

The goal of the higher order modulation operation is to make the bandwidth of each part as small as possible (Remember that narrower bandwidth means that larger sampling intervals can be applied. Using larger sampling intervals can reduce the number of sampling points).

The conventional modulation operation is to multiply the signal by a linear phase exponential function, as in (5). Here, instead of (5), we perform the generalized modulation operation and multiplying $x(t)$ by a higher order exponential function, i.e.,

$$x(t) \xrightarrow{\text{modulation}} m(t)x(t) \tag{6}$$

where

$$m(t) = \exp\left[j2\pi(a_n t^n + a_{n-1}t^{n-1} + \cdots\cdots + a_1 t + a_0)\right]. \tag{7}$$

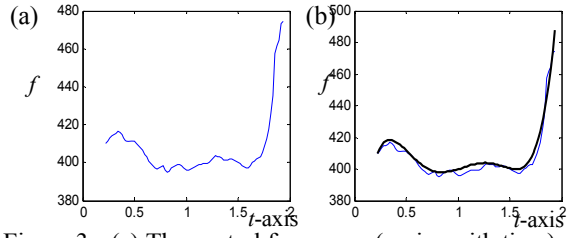

Figure 3 – (a) The central frequency (varies with time) of the whale voice signal whose STFT is as in Fig. 1(a). (b) Using a 5th order polynomial to approximate the central frequency of the whale voice.

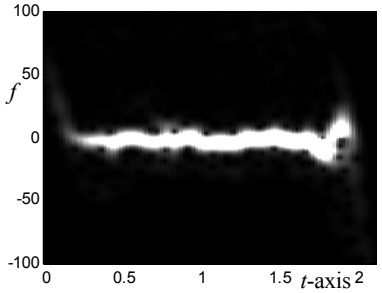

Figure 4 – The STFT of $x_2(t)$ where $x_2(t)$ is the result of **proposed high order modulation** of the analytic signal of the whale voice in Fig. 1(a) (***TF* value = 73.5**). Compared with Fig. 1(b), it can be seen that the bandwidth of $x_2(t)$ is much narrower than that of $x_1(t)$, which is generated from conventional modulation

Note that the phase of $m(t)$ is an n^{th} order polynomial. Since the instantaneous frequency of $m(t)$ is

$$\frac{d}{dt}(a_n t^n + a_{n-1}t^{n-1} + \cdots\cdots + a_1 t + a_0)$$
$$= na_n t^{n-1} + (n-1)a_{n-1}t^{n-2} + \cdots\cdots + a_1, \tag{8}$$

if $STFT_x(t, f)$ and $STFT_y(t, f)$ are the STFTs of $x(t)$ and $y(t) = m(t)x(t)$, respectively, then

$$STFT_y(t, f)$$
$$\cong STFT_x\left(t, f + na_n t^{n-1} + (n-1)a_{n-1}t^{n-2} + \cdots\cdots + a_1\right). \tag{9}$$

Therefore, with the generalized modulation in (7), one can adjust the "shape" of the time-frequency distribution of a signal more flexibly. It has higher ability to reduce the bandwidth requirement for a signal.

For example, for the whale signal whose STFT is as in Fig. 1(a), its central frequency is plotted as in Fig. 3(a). Note that the central frequency varies with time. Then, in Fig. 3(b), we use a 5th order polynomial as follows to approximate the central frequency curve in Fig. 3(a)

$$P_5(t) = 313.2 + 829.1t - 2298.6t^2 + 2728.5t^3$$
$$-1465.2t^4 + 292.9t^5. \tag{10}$$

The approximation is performed by Legendre polynomial expansion [9]. That is, if the central frequency of the signal is $h(t)$, then the n^{th} order polynomial used for approximating $h(t)$ can be determined from:

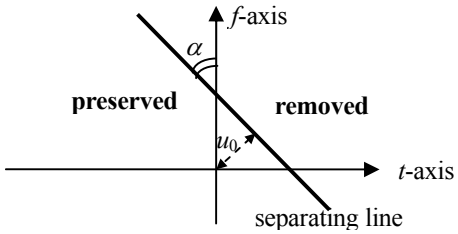

Figure 5 – The FRFT filter in (17) is equivalent to placing a separating line in the time-frequency domain.

$$P_n(t)=\sum_{k=0}^{n} a_k \phi_k(t) \quad \text{where } a_k=\int_{t_0}^{t_0+T} h(t)\phi_k(t)\,dt \text{ , (11)}$$

$$\phi_k(t)=\sqrt{\frac{2}{T}}L_k\left(\frac{t-t_0-T/2}{T/2}\right), \qquad (12)$$

$[t_0, t_0+T]$ is the support of $h(t)$, and $\{L_k(t) \mid k = 0, 1, 2, \ldots\}$ is the Legendre polynomial set that is orthonormal in the interval of $t \in [-1, 1]$. Since

$$\int P_5(t)\,dt = 313.2t + 414.5t^2 - 766.2t^3 + 682.1t^4 - 293.0t^5 + 48.8t^6, \qquad (13)$$

from (7)-(9), the whale voice signal can be modulated by

$$x_a(t) \xrightarrow{\text{modulation}} x_2(t)=m(t)x_a(t) \qquad (14)$$

where $x_a(t)$ is the analytic signal defined in (4) and

$$m(t)=\exp\left[-j2\pi\left(313.2t+414.5t^2-766.2t^3+682.1t^4-293.0t^5+48.8t^6\right)\right]. \qquad (15)$$

The STFT of $x_2(t)$ is plotted in Fig. 4. Compared with Fig. 1(b), it can be seen that the bandwidth of $x_2(t)$ is much narrower than the bandwidth of $x_1(t)$, which is generated from the conventional modulation operation. The **bandwidth** of $x_2(t)$ is only about **35 Hz** (from -17.5 Hz to 17.5 Hz) and the *TF* product is 35 × 2.1 = **73.5**. (Remember that the *TF* product is the lower bound of the number of sampling points). In comparison, the bandwidth of $x_1(t)$ is 100 Hz and its *TF* product is 210. Therefore, with the proposed higher order modulation operation, the bandwidth of a signal can be much reduced and the sampling efficiency is obviously improved.

3. COMBINING HIGHER ORDER MODULATION WITH THE FRACTIONAL FOURIER TRANSFORM

In [5][6][7][8], the fractional Fourier transform (FRFT) was adopted to rotate the time frequency distribution of a signal and improve the sampling efficiency. In this paper, we find that, combining the proposed higher order modulation with the FRFT, a very low sampling rate can be achieved.

In our signal sampling scheme, the FRFT plays two roles: "signal segmentation" and "bandwidth reduction".

To sample a signal adaptively, it is proper to separate a signal into several parts and choose a proper sampling interval for each part of the signal.

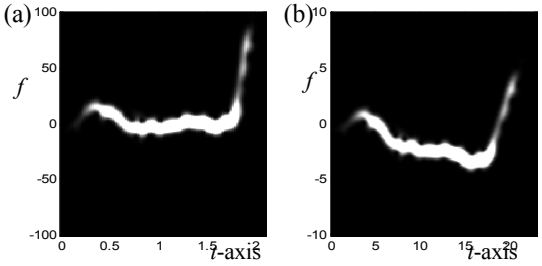

Figure 6 – (a) The STFT of the conventional modulation of the analytic signal for the whale voice. (b) After performing the FRFT and the scaling operation, the STFT is rotated.

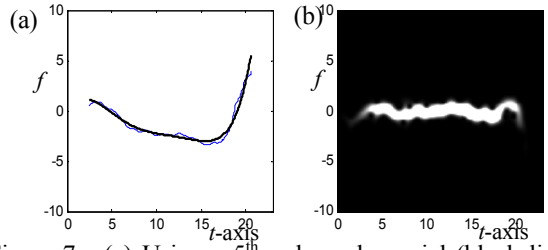

Figure 7 – (a) Using a 5th order polynomial (black line) to approximate the central frequency (blue line) of the signal in Fig. 6(b), (b) The STFT of the signal after **the scale FRFT + proposed high order modulation** (***TF* value = 50.4**).

Signal decomposition can be done by time-frequency analysis and the FRFT filter. The definition of the FRFT is:

$$O_{FRFT}^{\alpha}\left[x(t)\right] = \sqrt{1-j\cot\alpha}\int_{-\infty}^{\infty} e^{j\pi u^2\cot\alpha - j2\pi ut\csc\alpha + j\pi t^2\cot\alpha}\,x(t)\,dt. \qquad (16)$$

It can be viewed as performing the Fourier transform $2\alpha/\pi$ times. From [8], one can see that the FRFT has very close relations with the time-frequency distribution. If

$$y(t)=O_{FRFT}^{-\alpha}\left\{O_{FRFT}^{\alpha}\left[x(t)\right]H(u)\right\} \qquad (17)$$

where $H(u) = 1$ for $u < u_0$ and $H(u) = 0$ for $u > u_0$, then the FRFT filter in (17) is equivalent to placing a separating line in the time-frequency domain, as in Fig. 5. The angle between the line and *f*-axis is α and the distance between the line and the origin is u_0,

Moreover, the FRFT is also helpful for further reducing the bandwidth of a signal. Note that, for the whale signal in Fig. 1(b), the energy is large in a wide range when *t* is near to 2. Therefore, it is more proper to rotate the time-frequency distribution of the signal before performing higher order modulation for the signal. The rotation in the time-frequency domain can be done by the FRFT.

In Figs. 6(a) and 6(b), we show the STFTs of $x_1(t)$ and $x_3(t)$, respectively, where $x_1(t)$ is generated from (5) by choosing f_1 as 400 and $x_3(t)$ is the FRFT of $x_1(t)$. Here, the scaled operation is performed before applying the FRFT to balance the time domain and the frequency domain:

$$x_3(t)=O_{FRFT}^{0.2}\left[x_1(10t)\right]. \qquad (18)$$

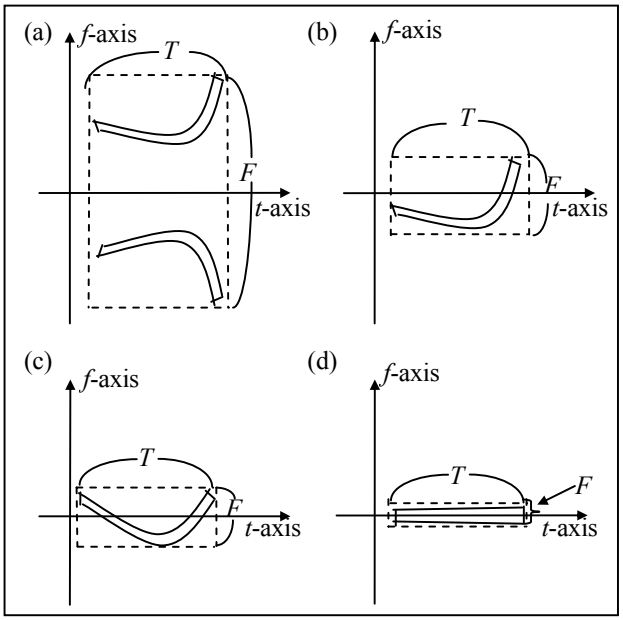

Figure 8 – The *TF* value, which reflects the lower bound of the number of sampling points, for each sampling algorithm. The *TF* value can be measured by the area of the block circled by the dot lines. (a) The original sampling algorithm. (b) Analytic signal conversion + modulation. (c) Analytic signal conversion + FRFT + modulation. (d) Analytic signal conversion + FRFT + **proposed higher order modulation**.

Then, according to the 5th order polynomial that can approximate the central frequency of $x_3(t)$, one can perform the following higher order modulation operation for $x_3(t)$:

$$x_3(t) \xrightarrow{\text{modulation}} x_4(t) = m(t)x_3(t), \tag{19}$$

$$m(t) = \exp\left[-j2\pi\left(-1.310t + 1.250t^2 - 0.281t^3 + 0.026t^4 - 0.001t^5 + 0.0002t^6\right)\right]. \tag{20}$$

The STFT of $x_4(t)$ is plotted in Fig. 7(b). In Fig. 7(b), the time support T is 21 and the bandwidth F is only 2.4. The value of *TF* product is only **50.4**, which is even less than that of Fig. 4.

In Fig. 8, the *TF* value (i.e., the area of the region circled by dash lines) for each sampling algorithm is shown. Remember that the *TF* value is the lower bound of the number of sampling points.

Since the analytic operation can remove the negative part, as in Fig. 8(b), and the FRFT can rotate the time frequency distribution of a signal, as in Fig. 8(c), they are helpful for reducing the number of sampling points. However, even in Fig. 8(c), the rectangular region circled by the dash lines still contains a lot of non-signal parts. Thus, it is proper to use the proposed higher order modulation scheme to "re-shape" the time-frequency distribution of the signal. After the proposed higher order modulation is applied, the *TF* product and hence the number of the required sampling points can be minimized, as in Fig. 8(d).

Table I. The actual numbers of sampling points (including the required extra parameters) and the reconstruction errors for sampling the whale voice signal in Fig. 1.

Sampling Algorithms	Actual Number of Sampling Points + Extra Parameters	Reconstruction error (by NMSE)
Convention	2137	0.607%
Analytic + Modulation	217	0.604%
Analytic + FRFT + Modulation	163	0.594%
Analytic + **Proposed High Order Modulation**	76	0.582%
Analytic + FRFT + **Proposed High Order Modulation**	60	0.581%

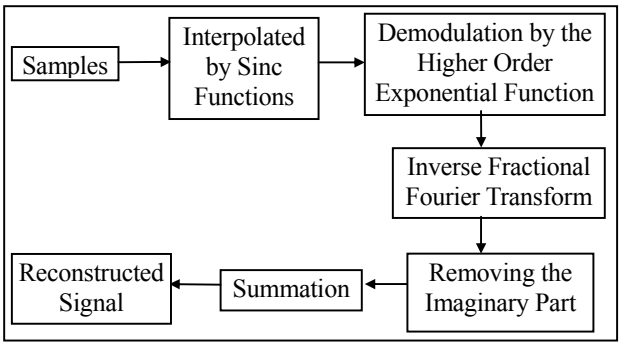

Figure 9 – The reconstruction process of the proposed sampling algorithm.

4. RECONSTRUCTION

The process of reconstructing the original signal, which is depicted in Fig. 9, is almost the same of that of the original sampling algorithm. The differences are that the signal should be demodulated by the higher order exponential function. Note that the sinc function interpolation is the inverse of the sampling operation and removing the imaginary part is the inverse of the analytic function generation operation.

For the whale signal in Fig. 1, the numbers of sampling points (including the extra parameters required for reconstruction, such as the coefficients of higher order modulation) and the reconstruction errors, which are measured by the NMSE (normalized mean square error) are shown. The result shows that the proposed high order modulation operation can indeed significantly reduce the number of sampling points without sacrificing the accuracy.

5. OTHER SIMULATIONS

In Table II, Figs. 10 and 11, and Table III, another two simulations are performed. The input signal for Table II is another whale voice signal acquired from [2].

Table II. The numbers of sampling points + extra parameters and the reconstruction errors for sampling another whale voice signal in [2].

Sampling Algorithms	Number of Sampling Points + Extra Parameters	Reconstruction error (by NMSE)
Convention	2192	0.737%
Analytic + Modulation	210	0.617%
Analytic + FRFT + Modulation	166	0.747%
Analytic + FRFT + **Proposed High Order Modulation**	93	0.554%

The input signal for Figs. 10-11 and Table III is a speech signal, which was acquired from a person who said the word "for". Both the simulation results show that the proposed higher order modulation operation is very helpful for improving the sampling efficiency for time-varying signals.

6. CONCLUSION

A new signal sampling algorithm, which is the combination of the higher order modulation operation, the STFT, and the FRFT filter is proposed. With the proposed algorithm, the number of sampling points is very near to the area of the nonzero region of the signal in the time-frequency plane, as the illustration in Fig. 8(d). From the simulation results, the proposed method requires much fewer number of sampling points to represent a signal. In addition to signal sampling, the proposed higher order modulation scheme is also helpful for improving the efficiency of data transmission and communication.

7. REFERENCES

[1] A. V. Oppenheim and R. W. Schafer, *Discrete-Time Signal Processing*, London: Prentice-Hall, 3rd ed., 2010.

[2] The whale voice data can be available from http:// oalib.hlsresearch.com/Whales/index.html.

[3] M. J. Bastiaans, "Gabor's Expansion of a Signal into Gaussian Elementary Signals," *Proc. IEEE*, vol. 68, pp. 594-598, 1980.

[4] K. Grochenig, *Foundations of Time-Frequency Analysis*, Birkhauser, Boston, 2001.

[5] H. M. Ozaktas, Z. Zalevsky, and M. A. Kutay, *The Fractional Fourier Transform with Applications in Optics and Signal Processing*, New York, John Wiley & Sons, 2000.

[6] T. Erseghe, P. Kraniauskas, and G. Carioraro, "Unified Fractional Fourier Transform and Sampling Theory," *IEEE Trans. Signal Processing*, vol. 47, no. 12, pp. 3419-3423, Dec. 1999.

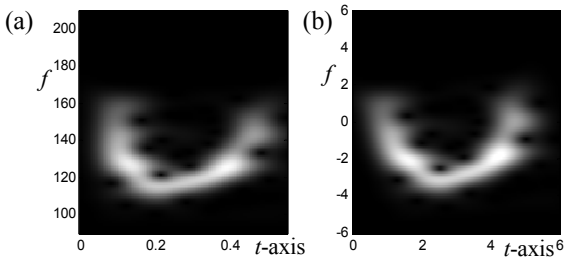

Figure 10 – (a) The STFT of the first harmonic part of the speech signal acquired from a person who said the word "for". (b) The STFT of the analytic signal conversion + conventional modulation + scaled FRFT operations for the speech signal in Fig. 10(a).

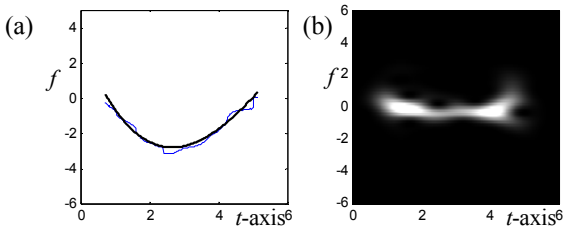

Figure 11 – (a) Using a 5th order polynomial (black line) to approximate the central frequency (blue line) of Fig. 10(b), (b) The STFT of the signal after high order modulation.

Table III. The numbers of sampling points + extra parameters and the reconstruction errors for sampling the speech signal in Fig. 10(a).

Sampling Algorithms	Number of Sampling Points + Extra Parameters	Reconstruction error (by NMSE)
Convention	173	4.199%
Analytic + Modulation	32	3.660%
Analytic + FRFT + Modulation	27	3.514%
Analytic + **Proposed High Order Modulation**	24	3.503%
Analytic + FRFT + **Proposed High Order Modulation**	21	2.870%

[7] R. Tao, B. Deng, W. Q. Zhang, and Y. Wang, "Sampling and Sampling Rate Conversion of Band Limited Signals in the Fractional Fourier Transform Domain," *IEEE Trans. Signal Processing*, vol. 56, no. 1, pp. 158-171, Jan. 2008.

[8] S. C. Pei and J. J. Ding, "Relations between Gabor Transforms and Fractional Fourier Transforms and Their Applications for Signal Processing," *IEEE Trans. Signal Processing*, vol. 55, no. 10, pp. 4839-4850, Oct. 2007.

[9] M. R. Spiegel, *Mathematical Handbook of Formulas and Tables*, McGraw-Hill, 1990.